

Numerical Calculation of Pressure Characteristics in Nozzle Flowmeter

Zi-Yan Hu, Sen-Da Qi, Jiang-Bo Tong, Feng Wang, Gong He,
Shu-Yuan Wang, Guo-Qing Zhao, Cheng-Xi Chai
College of Mechanical Engineering, Quzhou University, Quzhou, 324000, China;

ABSTRACT

In order to calculate the internal static pressure and total pressure of the nozzle flowmeter under different flow rates, the distribution law of internal static pressure and total pressure in the physical model of nozzle flowmeter under different flow values was explored by solving Navier-Stokes equations, pressure and velocity coupling. It is found that there is a close relationship between the static pressure inside the nozzle flowmeter and the total pressure characteristics and the change of flow rate. In the horizontal plane where the fluid flows through the upstream surface, downstream surface, outlet surface and the central axis of the nozzle flowmeter, the numerical variation law and pressure area are different on the four surfaces.

Keywords: *Nozzle flowmeter , Different flows , Static pressure distribution , Total pressure distribution*

Date of Submission: 24-11-2020

Date of Acceptance: 07-12-2020

I. INTRODUCTION

Flow measurement is widely used in various fields of industrial and agricultural production, national defense construction, scientific research, foreign trade, and people's lives. It is a relatively important system in industrial and municipal systems and an important basis for trade settlement and benefit analysis^[1]. Many scholars have conducted special research on nozzle flowmeter. Aiming at the non-standard application phenomenon of nozzle flowmeters, Liu Hongsheng through " Nozzle Flowmeter No-Standards Research " concluded that the flow calibration results under low working conditions are applicable to the full range range^[2]. Zhao Xiangyuan summarized the design, construction and application of nozzle type flowmeter in air separation based on various working conditions and problems encountered by Baosteel Gas^[3]. The article " Flow Field Numerical Simulation and Pressure Tapping Location Optimization of Nozzle Flow Meter " analyzes and studies the internal structure and flow field distribution of the nozzle, and proposes a plan for optimizing the position of the pressure taking port^[4]. Some scholars also discussed the flow measurement of natural gas^[5]. Wu Jinguang carried out further research on the flowmeter from the perspective of energy saving. Dong Hao, Zhu Xiaohui, and Wang Xining explored the application of energy-saving flow meters using calculation methods^[6]. Many scholars have also analyzed the pressure loss of the flowmeter. Fan Yulang, Meng Jiang, Zhao Yun, Li Xuezhong analyzed the pressure loss of the internal and external pipe differential pressure flowmeter and explored its energy saving^[7]. Zhang Lingfeng, Liu Tiejun, Xie Dailiang, and Xu Peng conducted an experimental study on the pressure loss of the double cone flowmeter^[8]. It is learned from the literature library that there is currently no clear published literature on the numerical value of the internal static pressure and total pressure distribution of the nozzle flowmeter, while this article focuses on the internal static pressure and total pressure distribution of the nozzle flowmeter. The value of is carried out related experiments and calculations.

II. RESEARCH OBJECTS AND METHODS

2.1 Physical model

The upstream surface of the nozzle flowmeter consists of a plane perpendicular to the axis, a contraction section with a 1/4 ellipse profile, a cylindrical throat, and possible grooves or bevels as shown in Figure 1. Its total length is 250 mm, the total width is 358 mm and the nominal diameter is 213 mm.

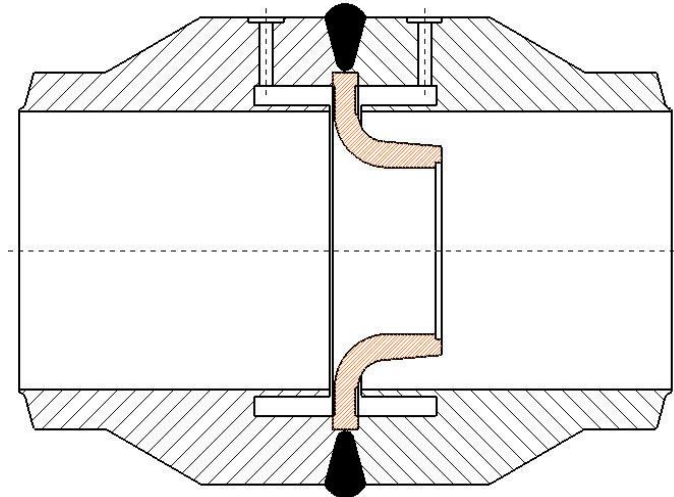


Figure 1 Overall structure of nozzle flowmeter

2.2 Governing equation

According to fluid mechanics, in the cartesian coordinate system, for incompressible viscous fluids, the law of motion is controlled by the Navier-Stokes equations. The forms of the continuous equation and momentum equation are as follows.

$$\frac{\partial \mu}{\partial x} + \frac{\partial v}{\partial y} = 0 \quad (1)$$

$$\rho u \frac{\partial u}{\partial x} + \rho v \frac{\partial u}{\partial y} = -\frac{\partial p}{\partial x} + \frac{\partial}{\partial y} \left(\eta \frac{\partial u}{\partial y} \right) \quad (2)$$

2.3 Calculation method

Under standard conditions, set the fluid properties, the fluid medium is water, and the density is 1 kg/m^3 , and the dynamic viscosity is $0.001 \text{ Pa} \cdot \text{s}$. In order to obtain accurate calculations, set the SIMPLE format for the coupled solution of pressure and velocity terms. Besides, for the purpose of eliminating the influence of the size effect brought by the standard nozzle forgings on the calculation results, set $\mu = U$, $v = 0$, which means set the standard nozzle core to the conditions of no penetration and no slippage.

2.4 Calculation plan

The surface identification of the key surface of the nozzle flowmeter has certain significance for the study of the internal flow characteristics. The face identification of the four faces is shown in Figure 2, where Face 1 represents the upstream face of the nozzle, Face 2 represents the downstream outlet face of the nozzle, Face 3 represents the outlet face of the nozzle flowmeter, and Face 4 represents the horizontal plane passing through the center axis of the nozzle flowmeter. The face line identification of the nozzle flowmeter is shown in Figure 3, where Line 11 is the centerline of the flowmeter.

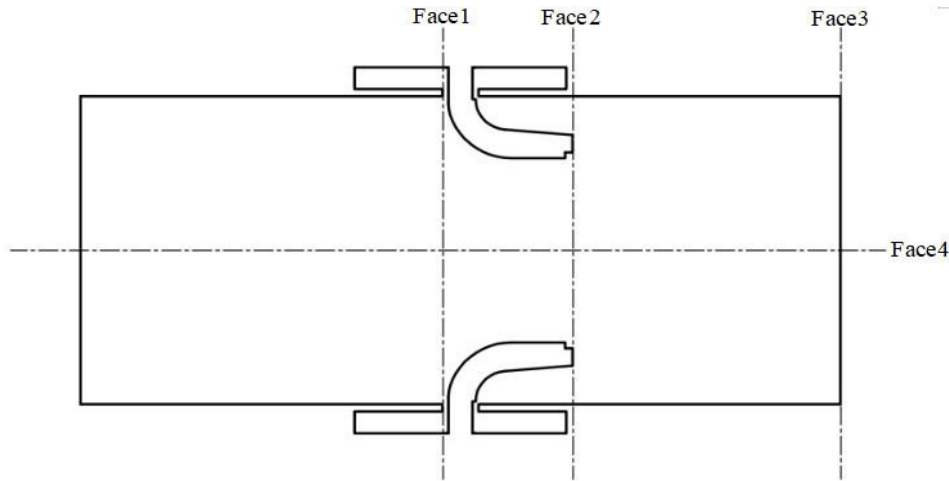


Figure 2 Nozzle flow meter surface identification diagram

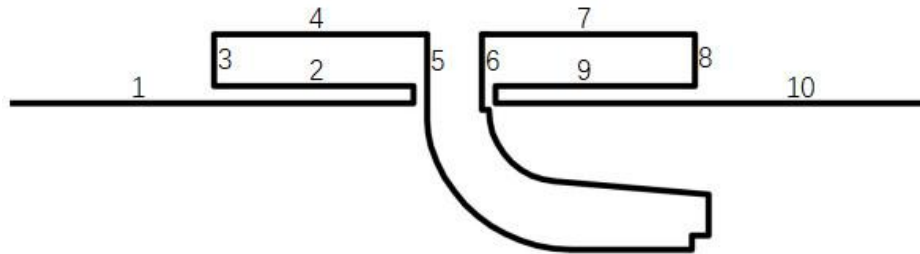


Figure 3 Nozzle flowmeter face line identification diagram

In order to study the distribution of static pressure and total pressure of nozzle flowmeter under different flow rates. This research will take 8 kinds of stable flow values, which are 5 m³/h, 25 m³/h, 50 m³/h, 125 m³/h, 250 m³/h, 500 m³/h, 750 m³/h and 1000 m³/h. The calculation scheme is shown in Table 1.

Table 1 Calculation scheme

Calculation plan (case)	No.1	No.2	No.3	No.4	No.5	No.6	No.7	No.8
Working condition flow (m ³ /h)	5	25	50	125	250	500	750	1000

For the study of 4 marking surfaces, the stable flow values are taken as 5 m³/h, 25 m³/h, 125 m³/h and 750 m³/h. Among them, 5 m³/h means ultra-small flow conditions, 25 m³/h means small flow conditions, 125 m³/h means medium and small flow conditions, and 750 m³/h means large flow conditions.

III. RESULT ANALYSIS

The (a), (b), (c) and (d) in the following cloud diagrams represent Face 1, Face 2, Face 3 and Face 4, respectively. The (a), (b), (c), (d), (e), (f), (g), (h), (i), (j), and (k) in the line drawing represent Line 1, Line 2, Line 3, Line 4, Line 5, Line 6, Line 7, Line 8, Line 9, Line 10 and Line 11.

3.1 The internal static pressure distribution

The static pressure distribution of the nozzle flowmeter at the ultra-small flow rate (5 m³/h) is shown in Figure 4. When the inlet flow rate is 5 m³/h, the maximum static pressure of Face 1 appears on the outermost circle of this surface and its value is 0.0038 Pa, and the minimum static pressure appears on the innermost circle of this surface and its value is 0.0026 Pa. The pressure distribution gradually decreases from the outermost layer to the innermost layer; The maximum static pressure of Face 2 appears at the center of this face and its value is -0.0001 Pa, and the minimum static pressure appears at the center of this face and its value is -0.0007 Pa; The maximum static pressure of Face 3 is approximately 0.0005 Pa across the entire surface, and the minimum static pressure appears in a sparse distribution on this surface, and its value is 0.0002 Pa. In addition the minimum static pressure distribution is not very concentrated; The maximum static pressure of Face 4 appears at the two

ends away from the center axis of the nozzle flowmeter and its value is 0.004 Pa. The minimum static pressure appears at the end of the standard nozzle core and its value is -0.0005 Pa. As you can see from the figure, the static pressure around the standard nozzle core changes significantly, and its static pressure distribution has a hierarchical change.

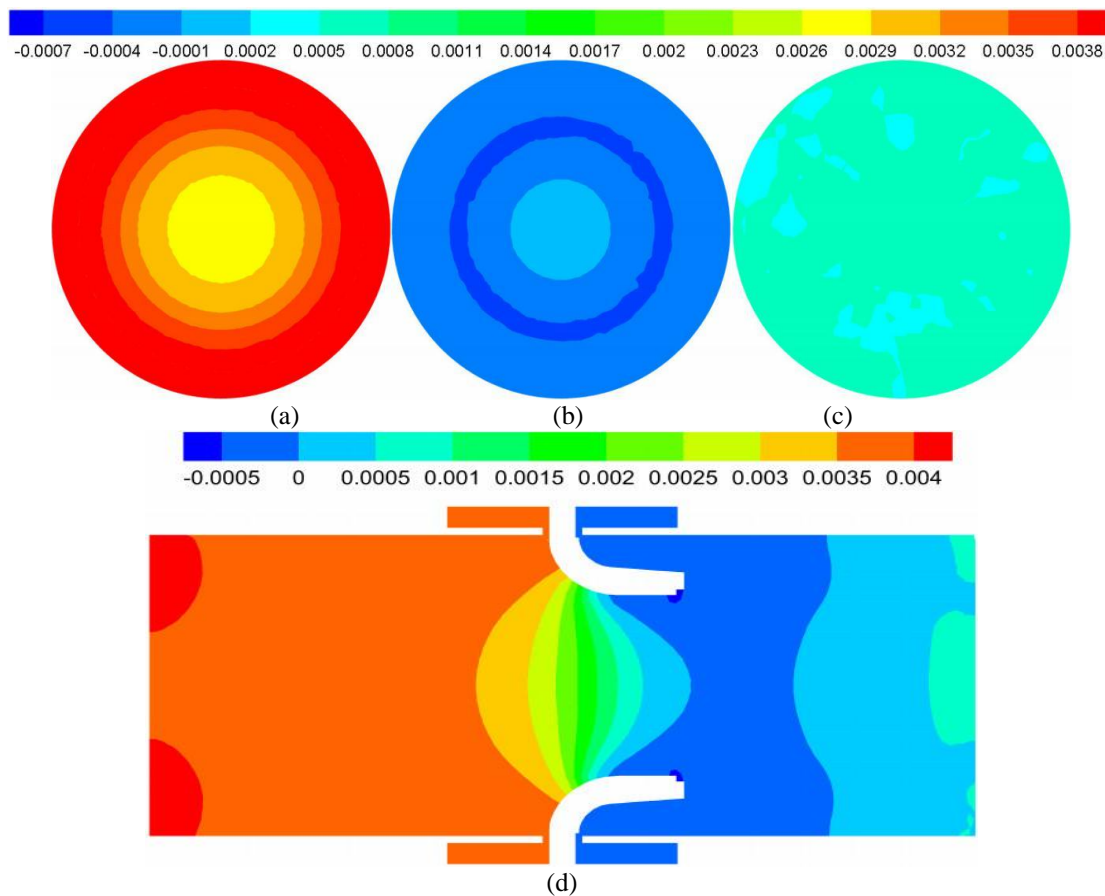


Figure 4 Static pressure distribution under ultra-small flow ($5 \text{ m}^3/\text{h}$)

The static pressure distribution of the nozzle flowmeter at a small flow rate ($25 \text{ m}^3/\text{h}$) is shown in Figure 5. When the inlet flow rate is $25 \text{ m}^3/\text{h}$, the maximum static pressure of Face 1 appears at the outermost circle of the nozzle upstream surface and its value is 0.078 Pa. The minimum static pressure appears at the center of this surface and its value is 0.048 Pa. The pressure distribution gradually decreases from the outermost layer to the innermost layer; The maximum static pressure of Face 2 appears at the exact center of the nozzle downstream outlet surface and its value is -0.002 Pa at the outermost circle. The minimum static pressure appears at the second circle of this surface and its value is -0.012 Pa. Its distribution is Compared with the flow rate of $5 \text{ m}^3/\text{h}$, the area occupied by the ring with the smallest static pressure becomes larger; The maximum static pressure of Face 3 appears at the exact center of the nozzle flowmeter outlet surface and its value is 0.018 Pa. The minimum static pressure mainly appears at the left edge of this surface and the two small points in the upper right corner with a value of -0.002 Pa; The maximum static pressure of Face 4 appears at the two corners of the nozzle flowmeter entrance and its value is 0.08 Pa, and the minimum static pressure appears in the part below the nozzle inflection point and its value is -0.01 Pa. The static pressure before the inlet of the standard nozzle core is relatively large, and the static pressure at the outlet is relatively small. As the flow rate increases, the static pressure at the outlet of the standard nozzle forging also shows a concentration phenomenon.

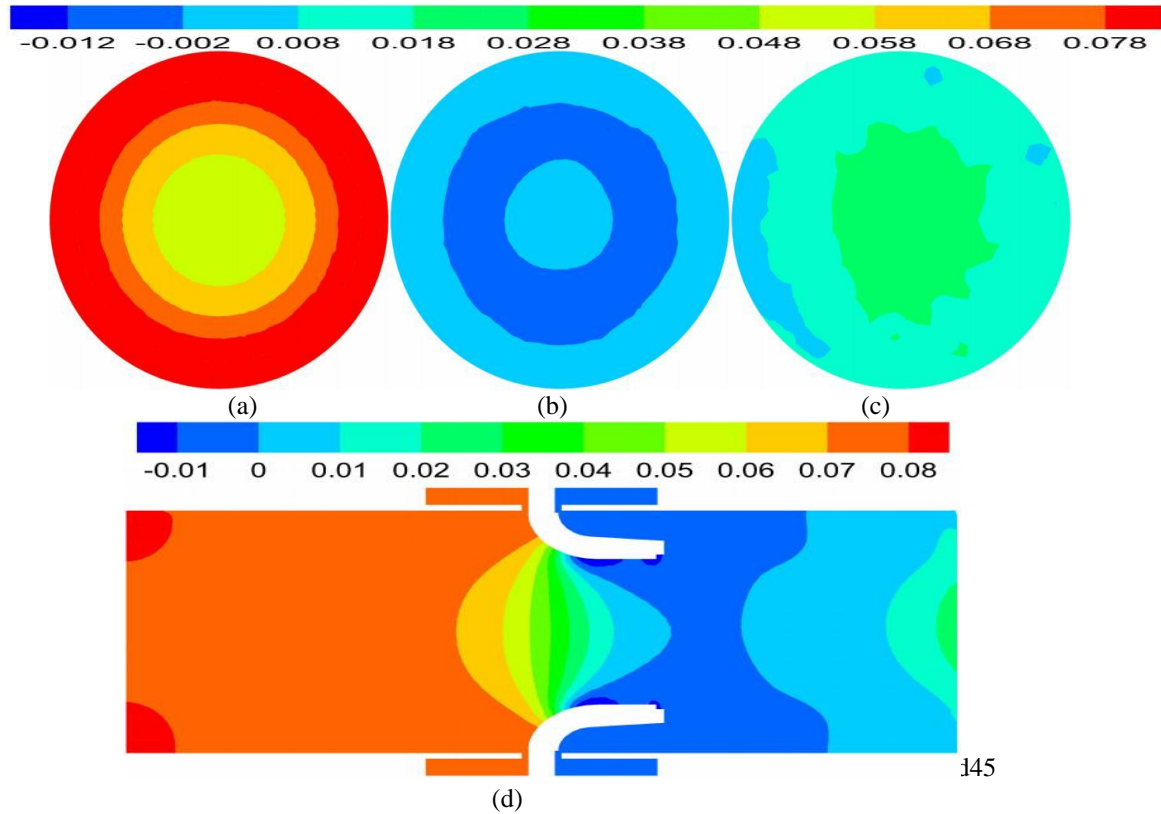
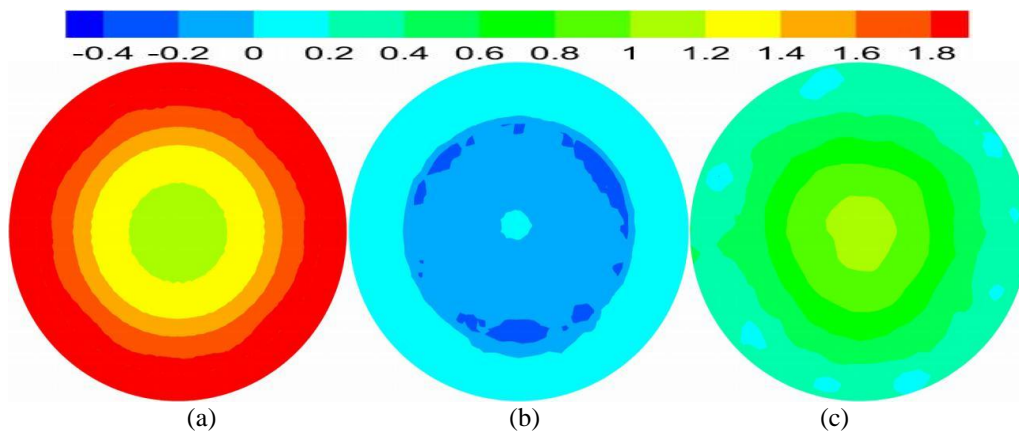


Figure 5 Static pressure distribution under small flow ($25 \text{ m}^3/\text{h}$)

The static pressure distribution of the nozzle flowmeter at the medium and small flow ($125 \text{ m}^3/\text{h}$) is shown in Figure 6. When the inlet flow rate is $125 \text{ m}^3/\text{h}$, the maximum static pressure of Face 1 appears at the outermost circle of this surface and its value is 1.8 Pa , and the minimum static pressure appears at the center of this surface and its value is 1 Pa . The static pressure gradually decreases from the outermost layer to the innermost layer. Compared with the small flow distribution, the static pressure distribution layer begins to increase; The maximum static pressure of Face 2 appears at the outermost circle and the center of the face with a value of 0 Pa , and the minimum static pressure appears sparsely on the edge of the center circle with a value of -0.4 Pa ; The maximum static pressure of Face 3 appears at the center of the nozzle flowmeter outlet surface and its value is 1.2 Pa , and the minimum static pressure is scattered at the outermost circle of this surface and its value is 0 Pa . The general trend of static pressure is to decrease from the center to the outside; The maximum static pressure of Face 4 appears at the inlet of the nozzle flowmeter and its value is 1.6 Pa , and the minimum static pressure appears at the inflection point of the nozzle and its value is -0.6 Pa . There are more static pressure distribution levels at the inflection point of the standard nozzle core, and the concentrated static pressure at the exit of the standard nozzle forging is becoming more and more obvious.



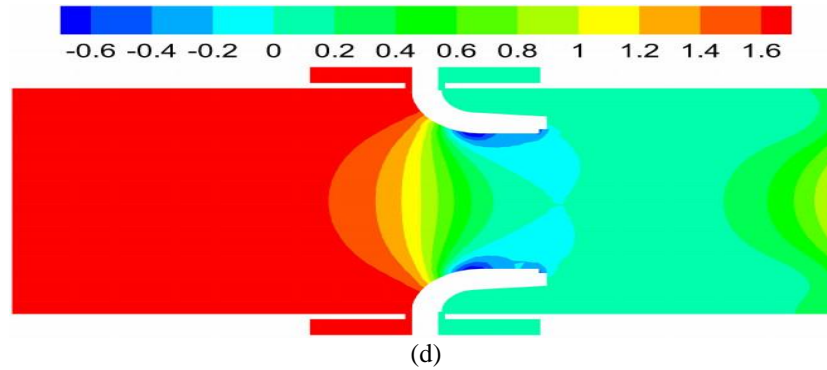


Figure 6 Static pressure distribution under medium and small flow ($125 \text{ m}^3/\text{h}$)

The static pressure distribution of the nozzle flowmeter at a large flow rate ($750 \text{ m}^3/\text{h}$) is shown in Figure 7. When the inlet flow rate is $750 \text{ m}^3/\text{h}$, the maximum static pressure of Face 1 appears at the outermost circle of the nozzle upstream surface and its value is 64 Pa, and the minimum static pressure appears at the second circle of this surface and its value is 44 Pa. Its static pressure gradually decreases from the outermost layer to the innermost layer; The large-area distribution of the maximum static pressure of Face 2 appears on the downstream outlet surface of the nozzle and its value is -6 Pa, and the small-area distribution of the minimum static pressure appears at the center of this surface and its value is -16 Pa; The maximum static pressure of Face 3 appears at the center of the outlet surface of the nozzle flowmeter and its value is 44 Pa, and the minimum static pressure appears at the top of this surface and its value is -6 Pa; The maximum static pressure of Face 4 appears at the inlet of the nozzle flowmeter and its value is 60 Pa, and the minimum static pressure appears at the inflection point of the nozzle arc and its value is -20 Pa. Compared with the previous flow rate, the static pressure distribution area at the outlet of the standard nozzle forging is getting smaller and smaller, and the static pressure is becoming more and more concentrated. The static pressure at the inlet of the standard nozzle core is affected by the static pressure change and the he pressure values are relatively large.

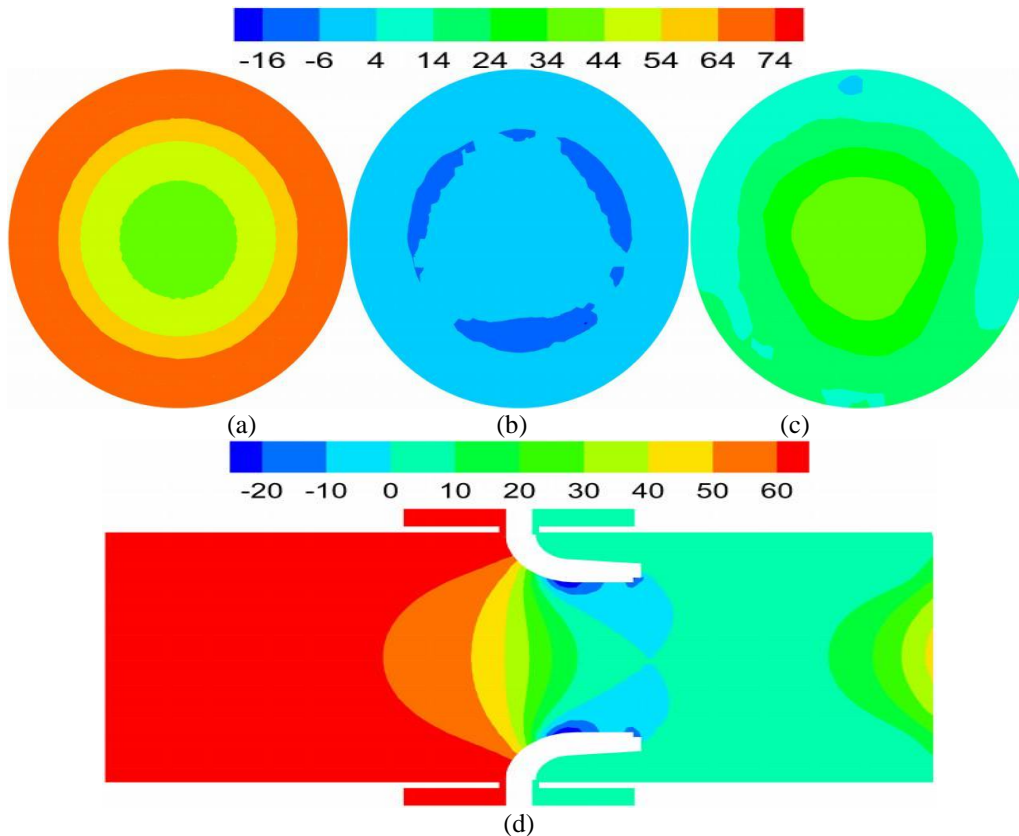


Figure 7 Static pressure distribution under large flow ($750 \text{ m}^3/\text{h}$)

3.2 The static pressure distribution at the boundary

The static pressure distribution of the nozzle flowmeter at the boundary is shown in Figure 8. Nozzle flow meters show different degrees of movement on different fluid surface lines, so the static pressure characteristics of each fluid surface line will still be different.

In Figure 8(a), Line 1 is basically not subject to static pressure at a small flow rate, and the static pressure is 0 kPa; when the flow is 125 m³/h, the static pressure is 2 kPa; when the flow is 250 m³/h, the static pressure is 7.5 kPa; when the flow rate is 500 m³/h, the static pressure is 28 kPa and there is a small increase trend; when the flow rate is 750 m³/h, the static pressure is 62 kPa and there is a slight increase trend; when the flow rate is 1000 m³/h, the static pressure is 112 kPa and has a large tendency.

In Figure 8(b), Line 2 is basically not subject to static pressure at a small flow rate, and the static pressure is 0 kPa; when the flow is 125 m³/h, the static pressure is 2 kPa; when the flow is 250 m³/h, the static pressure is 8 kPa; when the flow is 500 m³/h, the static pressure is 30 kPa; when the flow rate is 750 m³/h, the static pressure is 68 kPa; when the flow rate is 1000 m³/h, the static pressure is 120 kPa.

In Figure 8(c), Line 3 is basically not subject to static pressure at a small flow rate, and the static pressure is 0 kPa; when the flow rate is 125 m³/h, it is subject to static pressure 2 kPa; when the flow rate is 250 m³/h, it is subject to static pressure 8 kPa; when the flow is 500 m³/h, the static pressure is 30 kPa; when the flow is 750 m³/h, the static pressure is 68 kPa; when the flow is 1000 m³/h, the static pressure is 120 kPa.

In Figure 8(d), Line 4 is basically not subject to static pressure at a small flow rate, and the static pressure is 0 kPa; when the flow rate is 125 m³/h, it is subject to static pressure of 2 kPa; when the flow rate is 250 m³/h, it is subject to static pressure of 8 kPa; when the flow rate is 500 m³/h, the static pressure is 30 kPa; when the flow rate is 750 m³/h, the static pressure is 68 kPa; when the flow rate is 1000 m³/h, the static pressure is 120 kPa.

In Figure 8(e), Line 5 is basically not subject to static pressure at a small flow rate, and the static pressure is 0 kPa; when the flow rate is 125 m³/h, it is subject to static pressure 2 kPa; when the flow rate is 250 m³/h, it is subject to static pressure 8 kPa; when the flow is 500 m³/h, the static pressure is 30 kPa; when the flow is 750 m³/h, the static pressure is 68 kPa; when the flow is 1000 m³/h, the static pressure is 120 kPa.

In Figure 8(f), Line 6 is basically not subject to static pressure at a small flow rate, and the static pressure is 0 kPa; when the flow rate is 250 m³/h, it is subject to static pressure of 0.2 kPa; when the flow rate is 500 m³/h, it is subject to static pressure of 1.6 kPa. When the flow rate is 750 m³/h, the static pressure is 3.6 kPa, and when the flow rate is 1000 m³/h, the static pressure is 7.2 kPa and there is a slight downward trend.

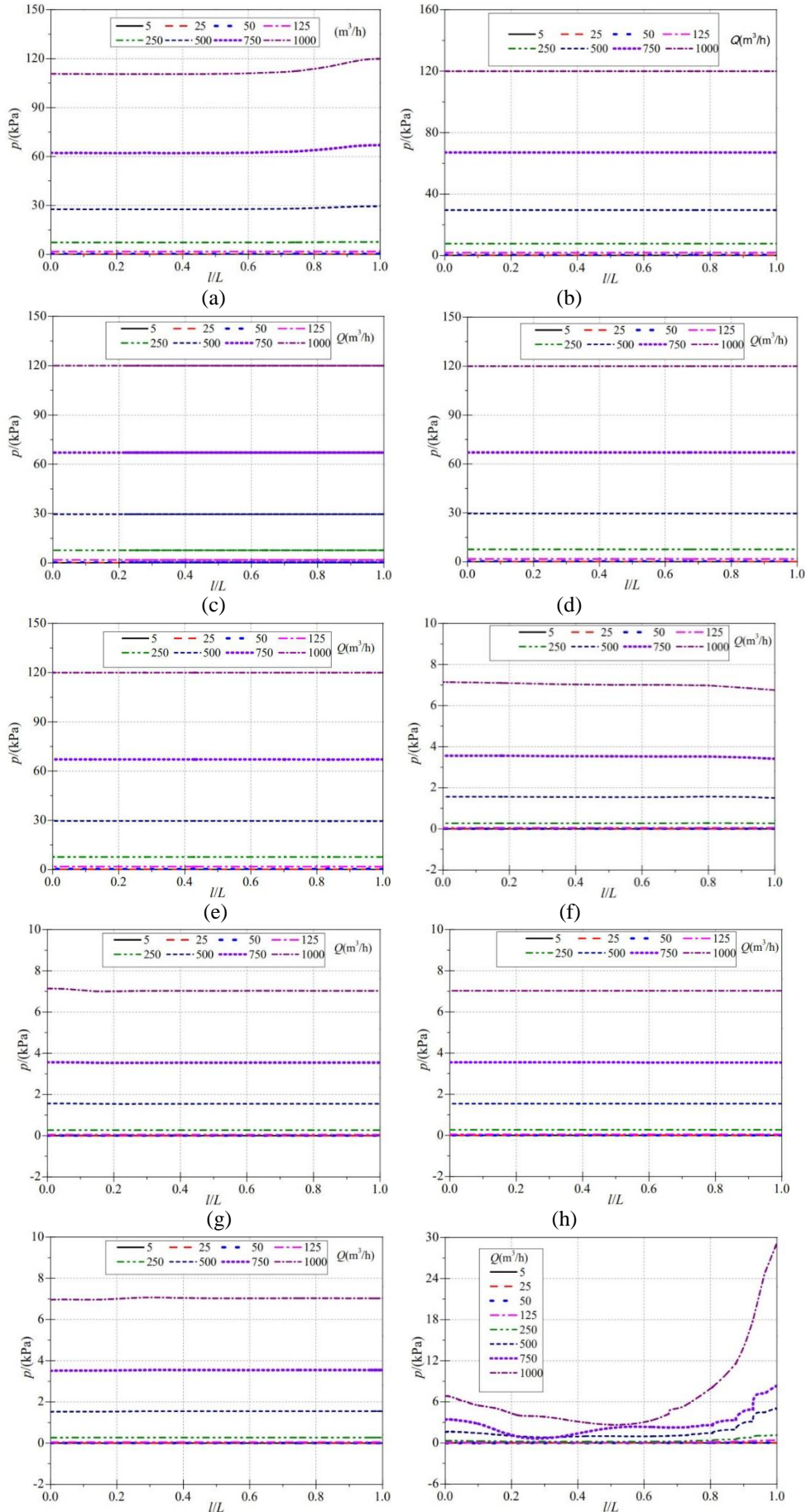
In Figure 8(g), Line 7 is basically not subject to static pressure at a small flow rate, and the static pressure is 0 kPa; when the flow rate is 250 m³/h, the static pressure is 0.2 kPa; when the flow rate is 500 m³/h, the static pressure is 1.6 kPa. When the flow rate is 750 m³/h, the static pressure is 3.6 kPa, and when the flow rate is 1000 m³/h, the static pressure is 7.2 kPa.

In Figure 8(h), Line 8 is basically not subject to static pressure at a small flow rate, and the static pressure is 0 kPa; when the flow rate is 250 m³/h, the static pressure is 0.2 kPa; when the flow rate is 500 m³/h, the static pressure is 1.6 kPa. When the flow rate is 750 m³/h, the static pressure is 3.6 kPa, and when the flow rate is 1000 m³/h, the static pressure is 7.2 kPa.

In Figure 8(i), Line 9 is basically not subject to static pressure at a small flow rate, and the static pressure is 0 kPa; when the flow rate is 250 m³/h, it is subject to static pressure of 0.2 kPa; when the flow rate is 500 m³/h, it is subject to static pressure of 1.6 kPa. When the flow rate is 750 m³/h, the static pressure is 3.6 kPa, and when the flow rate is 1000 m³/h, the static pressure is about 7 kPa.

In Figure 8(j), the static pressure on Line 10 first decreases and then increases. When the flow rate is 1000 m³/h, the change is the largest and most obvious. When the flow rate is 250 m³/h, when l is greater than 0.8 and less than 1, the static pressure on line 10 fluctuates; the flow rate is 500 m³/h, and the static pressure at the beginning is maintained at about 1.5 kPa, and then when l is greater than 0.8 and less than 1, the static pressure gradually rises to 4.6 kPa; the flow rate is 750 m³/h, the static pressure experienced fluctuates, and then reaches the top value, the static pressure is 8 kPa; with a flow of 1000 m³/h, the static pressure on Line 10 first decreases to the minimum value, which is 3 kPa, and then as l increases, the static pressure gradually increases to 29 kPa.

In Figure 8(k), the static pressure on Line 11 generally decreases and then increases. When l is 0, the initial static pressure values for 125 m³/h, 250 m³/h, 500 m³/h, 750 m³/h and 1000 m³/h are 2 kPa, 8 kPa, 28 kPa, 62 kPa and 111 kPa. The static pressure of line 11 under different flow rates decreases to 0 when l is 0.65, and then gradually increases. When the flow rate is 250 m³/h, 500 m³/h, 750 m³/h and 1000 m³/h, it increases to 4 kPa, 20 kPa, 42 kPa and 68 kPa.



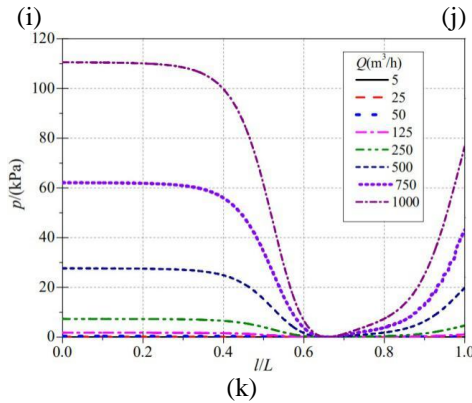


Figure 8 Static pressure distribution on the boundary

3.3 The total pressure distribution

The total pressure distribution of the nozzle flowmeter at the ultra-small flow rate ($5 \text{ m}^3/\text{h}$) is shown in Figure 9. When the inlet flow rate is $5 \text{ m}^3/\text{h}$, the maximum total pressure of Face 1 appears at the center of this surface and its value is 0.0042 Pa , and the minimum total pressure appears on the outermost circle of this surface and its value is 0.0036 Pa ; The maximum total pressure of Face 2 appears at the center of this face and its value is 0.0045 Pa , and the minimum total pressure appears on the outermost circle of this face and its value is 0 Pa ; The maximum total pressure of Face 3 appears at the center of this surface and its value is 0.0042 Pa , and the minimum total pressure appears at the outermost circle of this surface near the boundary and its value is 0.0003 Pa ; The maximum total pressure of Face 4 appears at the corners of both ends of the nozzle flowmeter inlet and its value is 0.0042 Pa , and the minimum total pressure appears at the right side of the nozzle flowmeter and its value is 0.0003 Pa .

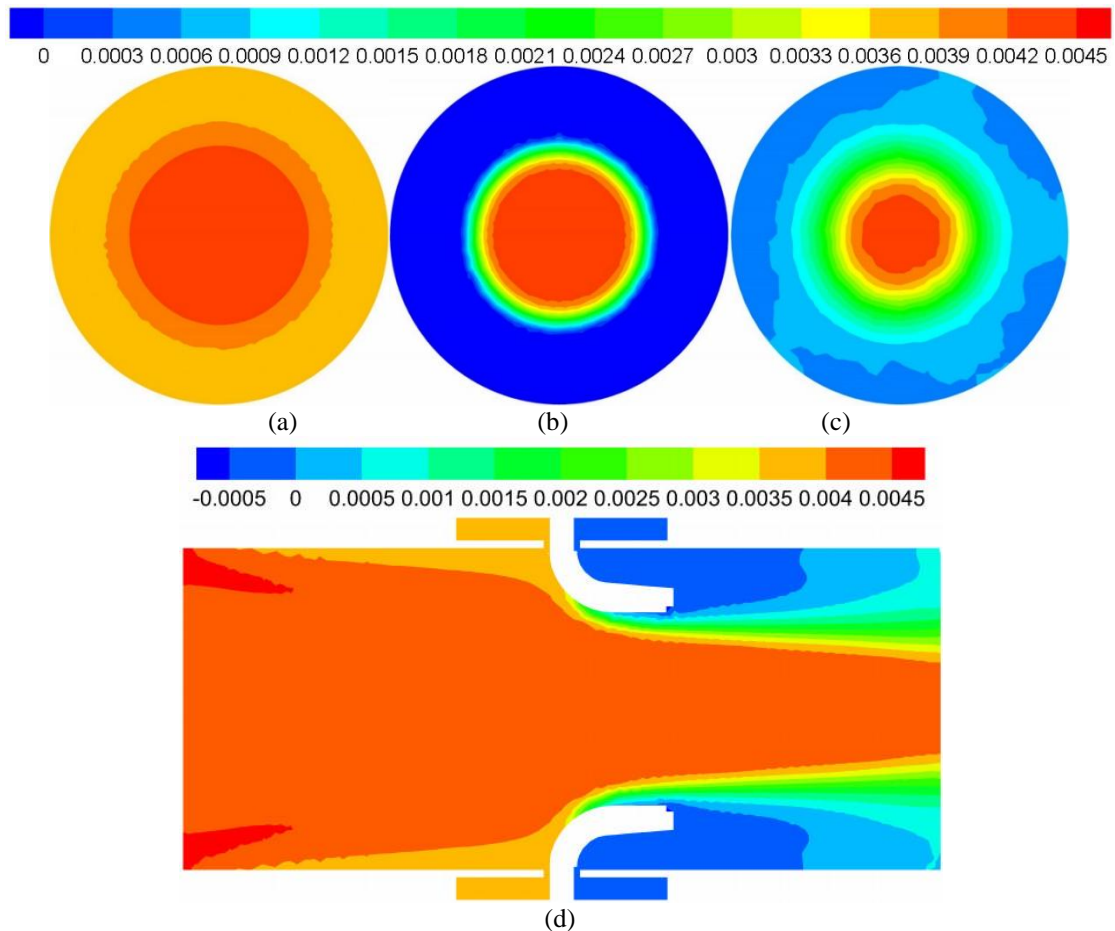


Figure 9 Total pressure distribution under ultra-small flow ($5 \text{ m}^3/\text{h}$)

The total pressure distribution of the nozzle flowmeter at a small flow rate ($25 \text{ m}^3/\text{h}$) is shown in Figure 10. When the inlet flow rate is $25 \text{ m}^3/\text{h}$, the maximum total pressure of Face 1 appears at the exact center of the nozzle upstream surface and its value is 0.09 Pa , and the minimum total pressure appears on the outermost circle of this surface and its value is 0.07 Pa . The total pressure is reduced from the innermost layer to the outermost layer, and the total pressure distribution is relatively simple; The maximum total pressure of Face 2 appears at the exact center of the nozzle downstream outlet surface and its value is 0.09 Pa . The minimum total pressure appears on the outermost circle of this surface and its value is 0 Pa . The total pressure decreases from the innermost circle. To the outermost layer, the total pressure distribution is more complicated, but it has certain rules; The maximum total pressure of Face 3 appears at the center of the nozzle flowmeter outlet surface and its value is 0.08 Pa . The minimum total pressure appears at the outermost boundary of this surface and its value is 0 Pa . The overall total pressure distribution has a certain law and the phenomenon of partial changes in total pressure; The maximum total pressure of Face 4 appears when the nozzle flowmeter flows out of the nozzle from the inlet and its value is 0.09 Pa . The minimum total pressure appears on the right side of the nozzle flowmeter and its value is -0.01 Pa . The total pressure value of is relatively large, especially the total pressure value of the path of liquid flow is around 0.08 Pa .

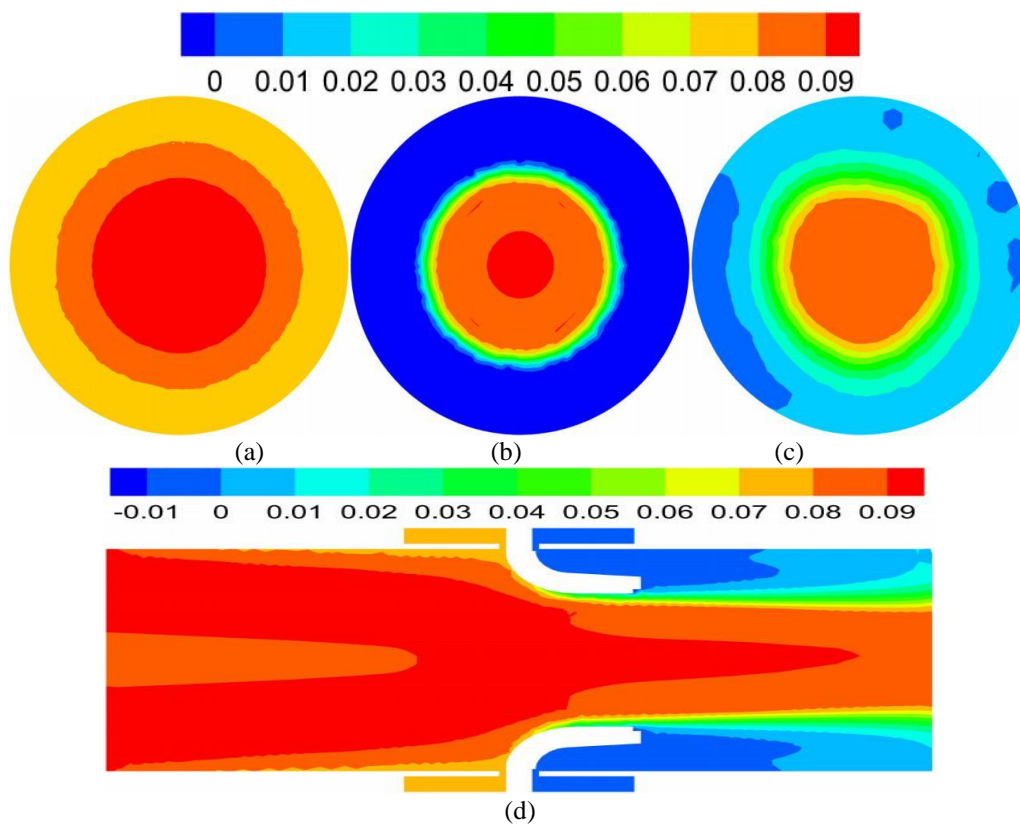


Figure 10 Total pressure distribution under small flow ($25 \text{ m}^3/\text{h}$)

The total pressure distribution of the nozzle flowmeter under medium and small flow ($125 \text{ m}^3/\text{h}$) is shown in Figure 11. When the inlet flow rate is $125 \text{ m}^3/\text{h}$, the maximum total pressure of Face 1 appears in the center of this surface and its value is 2 Pa , and the minimum total pressure appears in the outermost circle of this surface and its value is 1.8 Pa , which is different from the previous one. The flow rate is reduced compared to the total number of pressure ring layers it receives; The maximum total pressure of Face 2 appears at the center of this face and its value is 1.8 Pa . The minimum total pressure appears on the inner layer of the outermost circle of this face and its value is -0.2 Pa . The total pressure also increases in local small areas. The maximum total pressure of Face 3 appears at the center of the nozzle flowmeter outlet surface and its value is 1.8 Pa . The minimum total pressure appears at the outermost circle of this surface and its value is 0 Pa at a small local area. The overall trend of the total pressure changes from the maximum to the minimum. And the central circle layer is reduced to the outermost circle layer by layer; The maximum total pressure of Face 4 appears in the flow path from the nozzle flowmeter inlet to the nozzle flowmeter outlet, and its value is 2 Pa . The minimum total pressure appears on the right side of the nozzle flowmeter and its value is 0 Pa , which is $25 \text{ m}^3/\text{h}$. In comparison, the distribution of the total pressure experienced by the liquid flow path is more regular, and the area subject to

the maximum total pressure has also increased a lot.

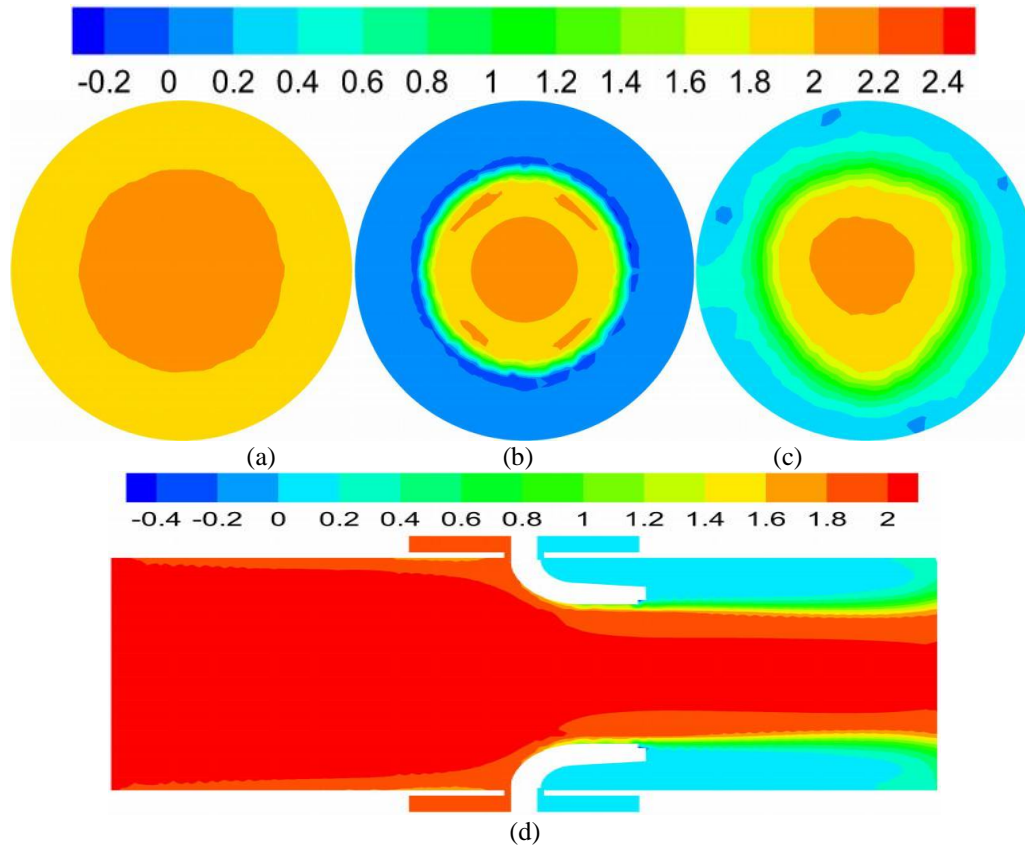


Figure 11 Total pressure distribution under medium and small flow ($125 \text{ m}^3/\text{h}$)

The total pressure distribution of the nozzle flowmeter at a large flow rate ($750 \text{ m}^3/\text{h}$) is shown in Figure 12. When the inlet flow rate is $750 \text{ m}^3/\text{h}$, the maximum total pressure of Face 1 appears at the second circle on the upstream surface of the nozzle and its value is 72 Pa, and the minimum total pressure appears at the outermost circle and the center of the face. At 64 Pa, compared with a flow of $125 \text{ m}^3/\text{h}$, the total pressure distribution increases by one more layer; The maximum total pressure of Face 2 appears at the exact center of the nozzle downstream outlet surface and its value is 72 Pa, and the minimum total pressure appears at the inner layer of the outermost circle of this surface and its value is 0 Pa. The overall trend of the total pressure gradually decreases from the innermost circle to the outermost circle; The maximum total pressure of Face 3 appears at the center of the nozzle flowmeter outlet and its value is 64 Pa, and the minimum total pressure appears at the small area of the outermost circle of this surface and its value is 0 Pa. The total pressure trend is also gradually reduced from the innermost circle to the outermost circle; The maximum total pressure of Face 4 appears on the path from the inlet of the nozzle flowmeter to the outlet and its value is 70 Pa, and the minimum total pressure appears on the right side of the nozzle flowmeter and its value is 0 Pa. It can be seen from the figure that compared with the previous flow rate, the area of the maximum total pressure received has increased.

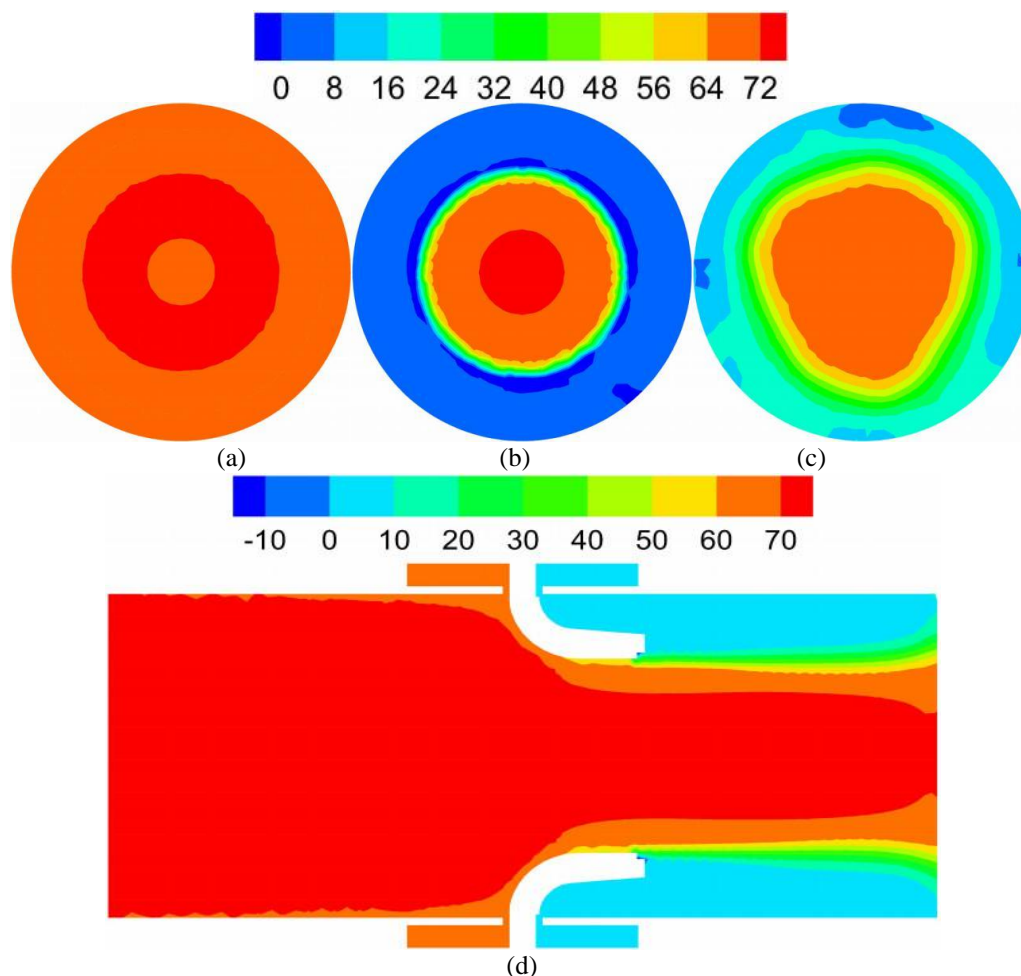


Figure 12 Total pressure distribution under large flow ($750 \text{ m}^3/\text{h}$)

IV. CONCLUSION

- 1) The static pressure and total pressure have the opposite distribution law on the upstream surface of the nozzle. The former decreases from the outside to the inside, and as the flow changes, the number of layers between the static pressure and the total pressure also changes.
- 2) When the internal static pressure and total pressure of the nozzle flowmeter are distributed on the downstream surface and the outlet surface, they all show a downward trend from the center to the outside. With the change of flow, the static pressure and total pressure are both at the minimum pressure on the corresponding surface. It has the characteristics of scattered distribution.
- 3) The static pressure and total pressure distribution on the horizontal plane of the center axis of the nozzle flowmeter change more obviously with the flow, but the total pressure distribution is more consistent and regular than the static pressure distribution.
- 4) The overall amplitude change of the static pressure on the upper boundary line of the nozzle and the center line of the flowmeter is larger than the other boundary lines.

ACKNOWLEDGEMENTS

The work was supported by the national college students' science and technology innovation project (No. 202011488018).

REFERENCES

- [1]. Wu Jinguang. Selection of flowmeter from the angle of energy saving[J]. Energy and Energy Conservation, 2019, (08): 65-66, 84.
- [2]. Liu Hongsheng. Nozzle flowmeter no-standards research[J]. Valve, 2014, (02): 7-8, 23.
- [3]. Zhao Xiangyuan. Application and analysis of nozzle flowmeter in air separation plant [J]. Internal Combustion Engine & Parts, 2018, (07): 70-72.
- [4]. Wang Yue, Yan Yongfei, Zhou Jianping, et al. Flow field numerical simulation and pressure tapping location optimization of nozzle flow meter[J]. Contemporary Chemical Industry, 2018, 47(10): 2161-2164, 2177.

- [5]. Zhang Fuyuan,Gao Jun,Wang Jingan.Analysis on the measurement of natural gas flow with standard nozzle flowmeter [J].China Metrology, 2016, (01): 96-100.
- [6]. Dong Hao,Zhu Xiaohui,Wang Xining.Energy analysis and calculation of energy-saving flowmeter [J]. Henan Chemical Industry, 2004, (08): 44-45.
- [7]. Fan Yulang,Meng Jiang,Zhao bing,et al. Pressure loss study on a new inside and outside tube differential pressure flowmeter [J].Machine Design & Research, 2014, 30(01): 98-100.
- [8]. Zhang Lingfeng,Liu Tiejun,Xie Dailiang,et al.Experimental research on the pressure loss of double-cone flowmeters [J].Journal of China University of Metrology, 2014, 25(02): 150-154, 203.

Zi-Yan Hu, Sen-Da Qi, et. al. "Numerical Calculation of Pressure Characteristics in Nozzle Flowmeter." *The International Journal of Engineering and Science (IJES)*, 9(11), (2020): pp. 44-56.